Investigation of Different Approaches to Real-Time Control of Prosthetic Hands With Electromyography Signals

João Olegário de Oliveira de Souza, Marcos Daniel Bloedow, Felipe Cezimbra Rubo, Rodrigo Marques de Figueiredo, Gustavo Pessin, and Sandro José Rigo, *Member, IEEE*

***Abstract*—In this article, we describe a real-time system for prosthetic hands control. The system architecture includes the integration of the electromyographic (EMG) signal acquisition devices, platform for the implementation of the real-time classifier, sensors for the detection of object slip after grasp and the open-source hand prosthesis. Three databases were used to evaluate the implemented classifiers: a database with EMG data from local volunteers and NinaPro DB2 and DB3 databases that include electromyography and accelerometry (ACC) data acquisitions. A Multilayer Perceptron (MLP) classifier was implemented on a platform for rapid prototyping (Raspberry Pi 3 model B+) and generated responses in real-time (11 ms) with average accuracy of 96.30% for 11 hand and wrist gestures/movements.**

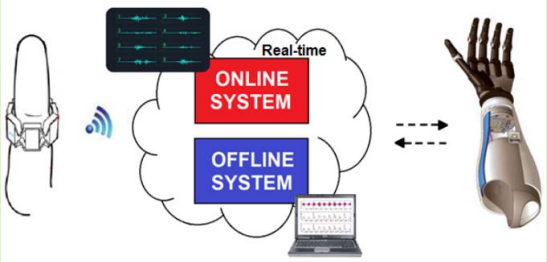

***Index Terms*—Electromyography, hand gesture recognition, machine learning, myoelectric prosthesis.**

I. Introduction

THE advances in engineering and computer science on the medical field enabled the development of lighter and adaptable prostheses. As regards inferior member prostheses, users of this equipment have even participated in high-performance sports. On the other hand, modern superior member prostheses, the myoelectric type, have five fingers and can achieve a high number of settings, though the hand's functional biomechanical complexity has kept these prostheses limited to restrained movements [1].

For the patient, the control over such equipment is still considered inadequate. The current systems have only one or two electrodes of surface electromyography. Therefore, complex sequences of muscular contraction's impulses need to be done to indicate the desired movement. In this context, it is not possible to carry out an intuitive control of the prosthesis [2, 3]. Besides, the high costs of some prosthetic models with better control features make them inaccessible for most of the amputees [3].

Two aspects are still widely explored by researchers in their studies on the control of upper limb prosthesis: EMG pattern recognition system [4, 5] and sensory feedback system [6-9]. For first aspect, several approaches and methodologies have been conducted and applied in the study of hand gesture recognition in order to improve the classifiers' performance.

Raurale and collaborators [4] present a combination of Linear Discriminant Analysis (LDA)-based projection Multilayer Perceptron (MLP) classification to exclude the

Manuscript received June 15, 2021; accepted July 7, 2021. Date of publication July 26, 2021; date of current version September 15, 2021. The associate editor coordinating the review of this article and approving it for publication was Dr. Varun Bajaj. *(Corresponding author: João Olegário de Oliveira de Souza.)*

This work involved human subjects or animals in its research. Approval of all ethical and experimental procedures and protocols was granted by the Institutional Research Committee through the Certificate of Presentation for Ethical Appreciation under Application No. 12038819.9.0000.5344.

João Olegário de Oliveira de Souza is with the Department of Electrical Engineering and the Department of Energy Engineering, Unisinos University, São Leopoldo 93022-000, Brazil (e-mail: jolegario@unisinos.br).

Marcos Daniel Bloedow is with the Department of Hardware and Software, Commbox Tecnologia, Porto Alegre 91330-010, Brazil (e-mail: marcosbloedow@gmail.com).

Felipe Cezimbra Rubo is with the Department of Research and Development, Altus Sistemas de Automação S.A., São Leopoldo, 93022-715, Brazil (e-mail: rubofelipe@gmail.com).

Rodrigo Marques de Figueiredo is with the Department of Electronics Engineering and the Department of Control and Automation Engineering, Unisinos University, São Leopoldo 93022-000, Brazil (e-mail: marquesf@unisinos).

Gustavo Pessin is with the Robotics Laboratory, Instituto Tecnológico Vale, Ouro Preto 35400-000, Brazil (e-mail: gustavo.pessin@itv.org).

Sandro José Rigo is with the Department of Computer Sciences, Unisinos University, São Leopoldo 93022-000, Brazil (e-mail: rigo@unisinos.br).

Digital Object Identifier 10.1109/JSEN.2021.3099744

redundant features from the feature set and identify nine wrist-hand movements. The method resulted in the classification rate that exceeds 99%.

Another approach uses other sensors, which can provide additional aspects in addition to electromyography (EMG), as presented in [10]. They used two sensors, comprising electromyography electrodes (EMG) and inertial measurement units (IMUs), to improve the performance of classification-based prosthesis control.

The use of commercial or open-source prosthetic models for online evaluation also fosters the opportunity for real tests to be performed, as exemplified in [11, 12]. Sattar *et al.* [13] developed an arm prosthesis control using a commercial platform to acquire EMG signals and the Raspberry system to process and control five movements/gestures, having the prosthetic arm's feedback signal with two levels of freedom. The offline training presented 94% accuracy using artificial neural networks. For the real-time analysis, the support vector machine (SVM) classifier implemented performed with 85% accuracy.

Sánchez-Velasco *et al.* [14] presented the use of an EMG commercial clamp to control an open-source hand prosthesis with six levels of freedom. The experiment used two portable, commercial hardware devices for the processing and actuation of the prosthesis. In this study, a classifier based on Extended Associated Memories (EAM) and the Median Absolute Value (MAV) was used to extract features. The robotic hand was tested in gesture recognition and grasp tasks. Results presented 95.83% accuracy.

In the context of development of sensory feedback system for myoelectric prosthetic hand, Weiner *et al.* [6] presented a scalable prosthesis prototype and a sophisticated multi-modal sensor system consisting of sensors for sensing normal and shear force, distance, acceleration, temperature, and joint angles. Zollo *et al.* [7] presented a real-time force and slippage closed-loop control employing tactile sensations via neural electrodes. During the closed-loop control, sensors embedded into the hand fingers were utilized to provide force and slippage information for the amputee subject. Cordella and collaborators [8] proposed and tested a real-time a system for object slippage detection during grasping and a control strategy for grasping force regulation and slippage prevention. The approach has been validated on a real prosthetic hand and three different objects for grasping. The system showed that it is able to perform a stable pinch grasp of different objects guaranteeing finger coordination. Prakash and Sharma [9] presented a low-cost system for force control of a custom-made myoelectric hand prosthesis using tactile sensor to estimate the contact force during finger-object interaction.

However, it is not easy to compare the results of different studies due to variations in the used evaluation methodologies and the different combinations of sensors. In this paper, we present hardware and software for real-time control of open-source hand prosthesis using EMG, slip and force sensors in the instrumentation and the machine learning to hand gesture recognition. Our approach contributes with improvements to support both the high accuracy in classification and the real time operation. The following architectures for the classification task were implemented and compared: Random Forest (RF) and Multilayer Perceptron (MLP) Neural Networks.

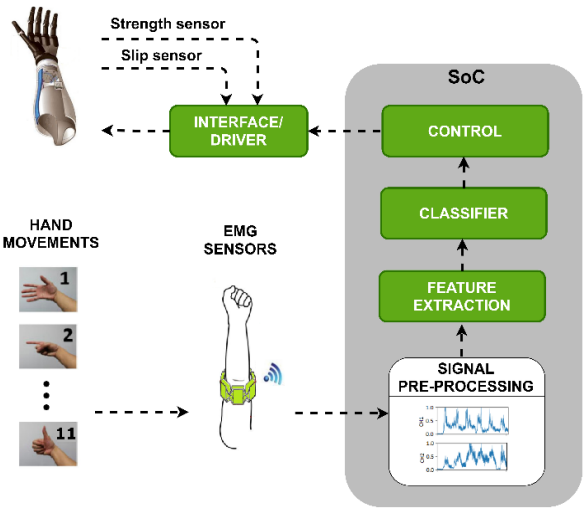

Fig. 1. Block diagram for hand prosthesis movement control.

After this introduction, the paper is divided into three sections. Section 2 proposes an online system with a brief description of the hardware and software. Section 3 presents the results of the assays and discussion. Finally, in section 4, we present the conclusions and outline future studies.

II. Methodology

Fig. 1 presents the components and the dynamics for the real-time actuation of an open-source prosthesis with electromyographic signal treatment through machine learning.

The online system uses a commercial platform for EMG signal acquisition and one low-cost System on Chip (SoC) platform for rapid prototyping. In this second platform, the classifier and other software elements (pre-processing, windowing and feature extraction) were implemented. The following routines were also created: real-time acquisition of EMG signals using Bluetooth communication, electric actuation of the hand prosthesis and signal feedback of sensors for monitoring and controlling strength and slip of objects inserted on the prosthetic hand during its grasp. These elements are described below.

A. Prototyping Platform

The classifier and firmware for communication with sensors and prosthesis' electric actuation were deployed/implemented on a 1.4 GHz ARM Cortex-A53 on the Raspberry Pi 3 B+ platform. The system was developed in the Python programming language 3.7 and the Tensorflow Lite tool was used for the classifier' development.

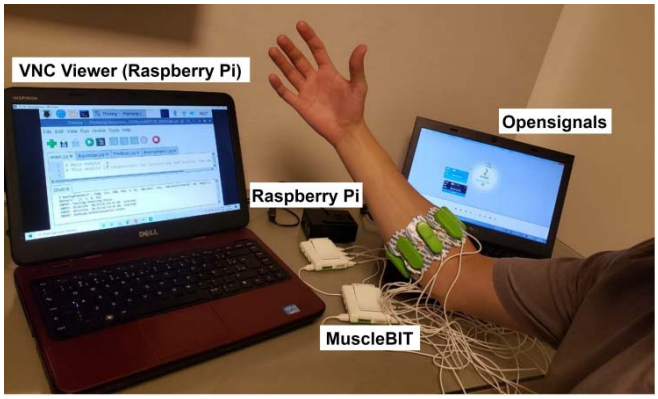

Fig. 2. Platform for EMG signal acquisition.

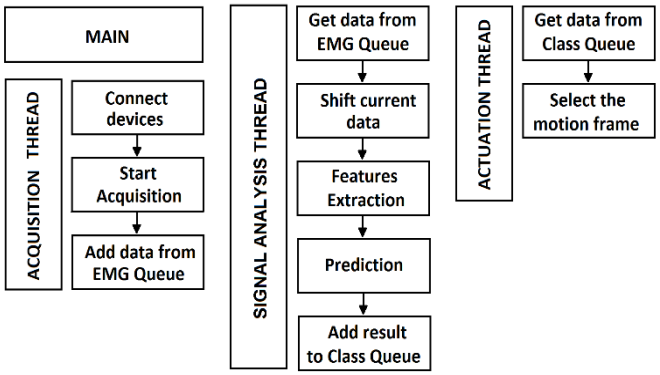

Fig. 3. Threads of process.

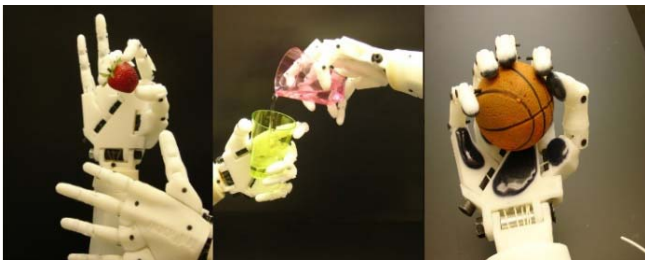

Fig. 4. Hand prosthesis' mechanical system.

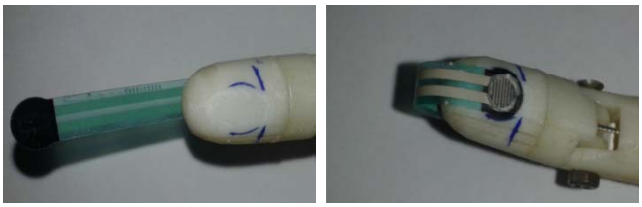

Fig. 5. FSR400 strength sensor and fixation.

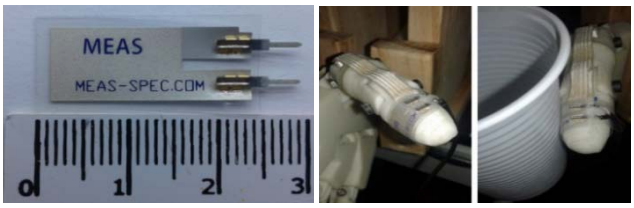

Fig. 6. LDT0-028K slip sensor.

B. System for EMG Signal Acquisition

For the acquisition of EMG signals, in the online stage, modules MuscleBIT from BITalino platform (PLUX – Wireless Biosignals S.A.) were used (Fig. 2). The acquisition of electromyographic signals is performed through surface electrodes, placed in an equally spaced way, around the forearm by two BITalino platforms. Each platform acquires four EMG signals at 1000 Hz and sends the results to the embedded system through Bluetooth communication.

C. Implemented Classifier for Online System

The best classifier was implemented on the SoC platform in three modules: Acquisition, Signal Analysis and Actuation. Each module runs a cyclic routine (thread) as shown in Fig. 3.

The acquisition module is responsible for establishing a Bluetooth connection with BITalino platform and starting the acquisition. EMG signals were acquired by the two BITalino platforms with 4 channels (each), summing up to 8 EMG channels. The values of the sampled channels are converted to a matrix together with the timestamp. This matrix is sent (queue) to the signal analysis module. The signal analysis module receives the samples, updates the window, extracts the features, classifies the movement and sends it to the prosthesis actuation module. The actuation module receives the classified gesture, selects the frame corresponding to the movement and sends to the prosthesis activation driver. Then, the slip monitoring function runs (external).

D. Prosthesis Prototype

The hand prosthesis used for object gripping tests is an adaptation of the open-source robotic platform project called InMoov, developed by French designer Gaël Langevin. The prosthesis (Fig. 4) has five fingers activated individually, summing up to five degrees of freedom (DoF).

Each finger is activated by a servomotor, enabling a finger-by-finger alternation of grasp strength. An interface between the prototyping platform and the servomotors was used for the electric drive.

E. Strength and Slip Sensors

The prosthetic hand's five fingers' pressure is monitored when it holds an object and may be detected when it slips. For this monitoring, slip and strength sensors are used. To quantify the pressure applied by the artificial finger on object manipulation, Inter-link Electronics' FSR400 strength sensor was used (Fig. 5). The force measurement system with FSR sensors was calibrated using a set of calibrated masses.

Slip sensors, responsible for detecting if an object is slipping from the fingers, are installed on the thumb and the index finger. The slip sensor used was LDT0-028K (Fig. 6), by Measurement Specialties. Schematic diagrams of the force and slip sensor signal conditioners are presented on Github repository described in the online supplementary material.

The simplified flowchart of the force and slippage system is showed in Fig. 7. The system starts the gripping movement and applies a minimum force to the object

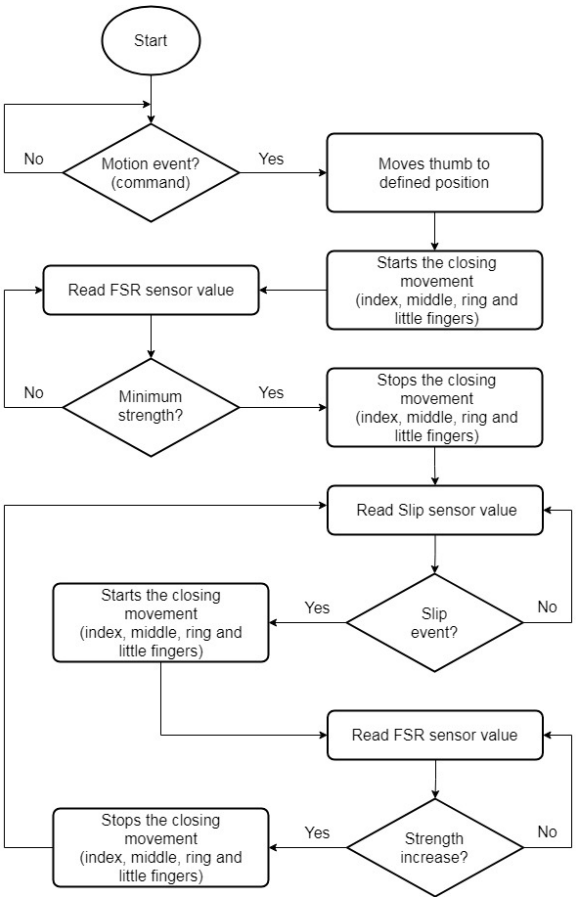

Fig. 7. Slippage system (signal conditioner output).

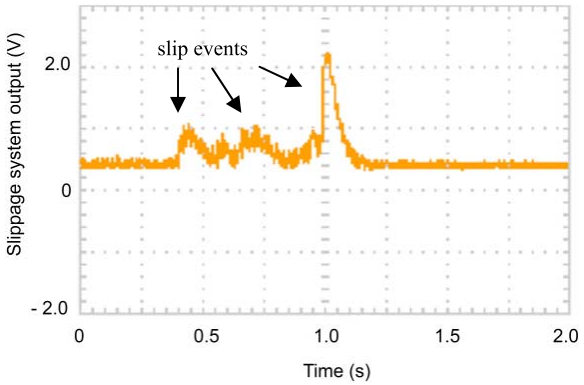

Fig. 8. Slippage system (signal conditioner output).

(empirical adjustment for each object) and it monitors if a slip event occurs. A threshold value is empirically determined to detect the onset of the slippage.

The slippage algorithm result will be a binary value 1 if a slippage event occurs and 0 if no slip event occurs. With the slippage detected, the system increments force value to output until a limit value. For simplicity, the class termination event does not appear. In this case, the prosthesis fingers open and the script returns to their starting point. Figure 8 illustrates the signal conditioner output of the slippage system when a slip event occurs.

Grip and slip tests were performed using three objects (Fig. 9): a plastic cup, a tennis ball (65 mm diameter and

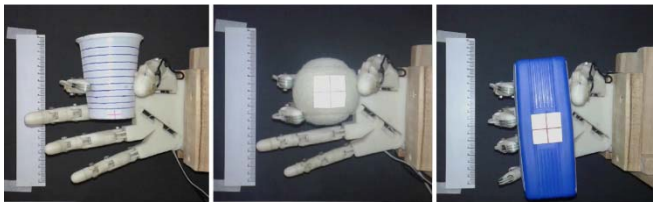

(a) plastic cup (b) ball 65 mm (c) plastic rectangle

Fig. 9. Objects for grip and slip tests.

58 g weight), and a plastic rectangle (150 mm x 50 mm x 30 mm size and 55 g weight).

In the first test with slippage system, an empty cup was placed in the prosthetic hand and then it was filled with water and compared the results with and without the slip monitoring system. For the other objects (tennis ball and plastic rectangle), a calibrated mass was placed on them. Tests were repeated 10 times for each object and to analyze the results, a video of each test was recorded and then checked frame by frame through video analysis software (Tracker).

F. Database for Training

Three databases were used to evaluate the implemented classifiers: NinaPro Database 2 and 3 (DB2 and DB3) and a database with EMG data from local volunteers.

The DB2 database includes EMG and accelerometry (ACC) data acquisitions of 40 intact subjects (12 females, 28 males; 34 right-handed, 6 left-handed). The DB3 database includes EMG and ACC data acquisitions of 11 transradial amputees (11 males: 10 right-handed, 1 left-handed). In these databases, each subject is required to perform 49 movements (8 isometric and isotonic hand configurations; 9 basic wrist movements; 23 grasping and functional movements and 9 force patterns). The EMG signals were acquired using 12 active electrodes in the differential pair setting (which provides a sampling rate of 2 kHz). A number of eight sensors were placed around the forearm, equally spaced, two electrodes were placed on the finger's flexing and extending muscles and two sensors were placed on the main activity spots of the biceps and triceps brachii [15]. Each electrode has a 3-axis accelerometer sampled at 148 Hz, which totals 36 channels. Each movement was repeated 6 times with a 3 second rest time in between [15, 16]. For this article, the first 10 subjects from the DB2 dataset and 10 subjects from the DB3 dataset were used. The subject 7 from DB3 was eliminated for all our analyses due presenting low classification accuracy (under 18%) in all tests. We consider the assays with 50 gestures/movements (including the resting position) for comparison with the existing literature.

For the third database, five intact adults (see Table I) volunteered for this investigation/experiment after providing signed informed consent (the UNISINOS University Ethical Committee approved all experimental procedures). The 11 hand and wrist gestures/movements that form our database, denoted KidoPro, were inspired by the work of Raurale and collaborators [4], Zhai *et al.* [17] and the NinaPro database DB2 [15].

The different movements performed interspersed by a rest class were: thumb up, hand closure, hand open, fine pinch grip, chuck grip, spherical grip, medium wrap, wrist pronation

TABLE I
DATABASE SUBJECT DESCRIPTION

Subject	Age (years)	Gender	Height (m)	Weight (kg)
1	40	M	1.75	75.0
2	41	M	1.74	68.0
3	40	F	1.65	73.0
4	36	M	1.85	78.0
5	33	F	1.56	57.0

TABLE II
MOVEMENTS USED FROM KIDOPRO DATABASE

Class	Description	Ninapro DB2 [16]	Raurale et al. [4]	Zhai et al. [18]
0	Rest	X	X	
1	Thumb up	X		
2	Hand closed	X	X	X
3	Hand opened	X	X	X
4	Fine pinch grip	X		X
5	Chuck grip	X		X
6	Spherical grip	X		
7	Medium wrap	X		
8	Wrist pronation	X	X	X
9	Wrist supination	X	X	X
10	Tool grip			X

and supination and tool grip (Table II). Our database has similar characteristics to the NinaPro DB2 (six repetitions of movements and all movements were alternated with an intermediate rest movement).

For the training stage, the database was recorded using the hardware described in Section II.B by Opensignals software (PLUX – Wireless Biosignals S.A.).

After acquiring the EMG signals, it was necessary to label where, in the data stream, a subject is performing each gesture/movement. The data were zero offset and bandpass-filtered.

Then, the Teager-Kaiser Energy Operator (TKEO) (1) was applied, obtaining a transformed signal $y(n)$ [18]:

$$y\,(n) = EMG_i^2 - EMG_{i+1}.EMG_i, \tag{1}$$

where EMG_i is the EMG signal and i is the sample number.

Subsequent to TKEO calculations, the $y(n)$ signal was rectified and filtered. The threshold value was defined according to the method proposed by Solnik *et al.* [18]. The leading channel (the one with the strongest signal) was selected and decided when a contraction starts and ends, consistently for all the eight channels. For comparison and validation, the visual inspection and the envelope detection methods were used. The envelope detection was designed for 7 Hz cutoff frequency and the threshold value empirically defined. Fig. 10 shows (a) the EMG signals (two channels), (b) the filtered and rectified signal $y(n)$ and (c) TKEO and Envelope methods.

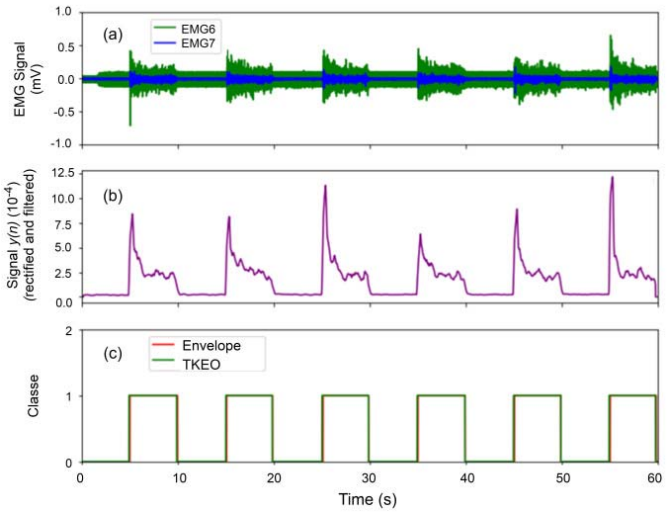

Fig. 10. EMG envelope detection and TKEO methods.

This first version of our database has been made available to download on repository https://github.com/eng-olegario/prosthesis-control.

G. EMG Features

Regarding the features to be extracted from the EMG signal, 15 time-domain (TD) features were tested using filter based statistical linear correlation (Pearson's Correlation Coefficients). This method is used to remove the irrelevant features [5]. In this paper we used seven TD functions that presented correlation coefficients less than 0.75: Mean Absolute Value (MAV), the Root Mean Square (RMS), and the Wave Length (WL), log Root Mean Square (logRMS), Variance (VAR), Kurtosis (KUR) and Skewness (SKEW) as presented in Table III [19], where N is the width of segmented window, EMG_i is the EMG signal sample, μ is the mean value of EMG and σ is the standard deviation of EMG.

Our approach used a total of 84 EMG features, with 7 functions in the TD and 12 EMG channels for DB2 and DB3 databases processing. For accelerometry signals, we employ the Mean Absolute Value function to calculate the features for this modality, as proposed by Fougner and collaborators [20]. Thus, we have 36 values of ACC features.

H. Data Processing

For hyperparameter optimization, training and test, the signals were segmented using a sliding window with a length of 200 samples (200 ms). The increment of the sliding window was set to 100 samples (100 ms). The same way as in the NinaPro study [16], the data for each subject was split into training and test sets based on repetitions. The second and fifth repetitions for each movement were used for the testing set, while the remaining four repetitions were used for the training set.

I. Feature Projection

The Feature Projection (also called dimensionality reduction) transforms data vectors from a high-dimension space onto a low-dimension space. Techniques such as Principal Components Analysis (PCA) and Linear Discriminant

TABLE III
TIME-DOMAIN FEATURES

Feature	Equation
Mean Absolute Value (MAV)	$\text{MAV} = \frac{1}{N}\sum_{i=1}^{N}\lvert EMG_i\rvert$
Root Mean Square (RMS)	$\text{RMS} = \sqrt{\frac{1}{N}\sum_{i=1}^{N}(EMG_i)^2}$
Wave Length (WL)	$\text{WL} = \sum_{i=1}^{N-1}\lvert EMG_{i+1} - EMG_i\rvert$
log Root Mean Square (logRMS)	$logRMS = log\left(\sqrt{\frac{1}{N}\sum_{i=1}^{N}(EMG_i)^2}\right)$
Variance (VAR)	$\text{VAR} = \frac{1}{N-1}\sum_{i=1}^{N}\lvert EMG_i - \mu\rvert$
Kurtosis (KUR)	$\text{KUR} = \frac{1}{N}\sum_{i=1}^{N}\left(\frac{EMG_i - \mu}{\sigma}\right)^4$
Skewness (SKEW)	$\text{SKEW} = \frac{1}{N}\sum_{i=1}^{N}\left(\frac{EMG_i - \mu}{\sigma}\right)^3$

Analysis (LDA) are used in the pre-processing step for pattern-classification applications [4]. Within linear projection, PCA maximizes the variance of data, whereas, LDA maximizes the separation between multiple classes and minimize the distance within classes simultaneously [4, 21]. The technique is outlined in the following steps:

1. Compute the mean feature vector $\bar{f}$ for the different classes from the dataset;
2. Compute the within-class scatter matrix and the between-class scatter matrix (covariance matrix in the case where PCA is used);
3. Select k eigenvectors that correspond to the k largest eigenvalues;
4. Construct the projection matrix L (P in the case where PCA is used) using top k eigenvectors;
5. Use the matrix L (or P) to transform the d-dimensional samples onto the new k-dimensional subspace. This can be summarized by (2):

$$Y_{n\times k} = X_{n\times d} L_{d\times k} \tag{2}$$

where a sample $X \in \mathbb{R}^{n\times d}$ (n and d are the number of samples and dimension of dataset respectively) can be projected onto the linear transformation matrix $L \in \mathbb{R}^{d\times k}$ ($P \in \mathbb{R}^{d\times k}$ in the case where PCA is used) to get a new sample $Y \in \mathbb{R}^{n\times k}$ (where $k \ll d$).

The LDA is most commonly used as dimensionality reduction technique for EMG classification systems [4]. In the experiments with EMG plus ACC, we reduce the dimension using LDA and PCA and comparing the results. The dimensionality (k) of output vector was chosen to be the number of classes minus one [21].

J. Implemented Classifiers for Offline System

For the first experiments, we performed an offline analysis investigating the performance of two classifiers (RF and MLP) by three databases processing (DB2 and DB3 NinaPro and KidoPro). The classifiers were implemented, trained and tested in a desktop computer based on a 64-bit Windows, equipped with Intel Core-i5 processor, with 1.6 GHz for processing and 6 GB memory. The system was developed in the Python programming language 3.7 and the Tensorflow and Scikit-Learn tools was used for the classifiers' development.

For the Random Forest classifier, three hyperparameters were adjusted during training by GridSearchCV. The number of decision trees was {10, 50, 100, 150, 200}, the maximum number of levels was {20, 50, 100, 150, 200} and the number of features to consider when looking for the best split {auto, square root}.

In the case of the MLP classifier, the number of hidden layers was determined by empirical observation. We considered two hidden layers with 600 and 200 neurons respectively. The function used was ReLu and Adam solver using 10% of the training data as validation. For output, a Softmax layer with 11, 12 or 50 neurons (number of classes) depending on the comparison. The training of the artificial neural network was performed in 100 epochs and all the network's biases and weights started with random values.

K. Evaluation and Statistical Analysis

Accuracy, presented in (3), was computed for evaluating the performance of our method and it is defined as:

$$Accuracy\,(\%) = \frac{\text{Correctly classified segments}}{\text{Total classified segments}} x100\% \tag{3}$$

All pairwise comparisons were based on one-way ANOVA followed by Bonferroni post-hoc analysis. Significant level was set at $p < 0.05$.

III. EXPERIMENT RESULTS AND DISCUSSION

A. Offline System Results

To validate and compare the classifiers with the existing literature, our baseline version and related papers used the DB2 and DB3 databases. The best scenario for each paper was considered. The average accuracies on all 50 movement types are presented in Table IV.

The average accuracy of our best classifier (in this case, RF classifier), considering on all 50 movement types for the DB2 database, was 75.88%, which is similar than the best results (75.27%) reported in Atzori and collaborators [23] using Random Forests and slightly less than the best result (78.71%) by Zhai *et al.* [17] with Convolutional Neural Network (CNN) classifier.

For DB3 database with 50 classes, our best result was also with the RF classifier that obtained an average classification accuracy of 56.08% (considering subject 7 from DB3, the accuracy was 53.61%). The values indicate that the analytic findings of this assay are relatively superior to the simple architectures presented by Atzori and collaborators [23] and relatively similar in terms of classification performance when compared to the best results by Zhai *et al.* [17] with

TABLE IV
THE AVERAGE CLASSIFICATION ACCURACY (%) FOR DIFFERENT PAPERS - DB2 AND DB3 NINAPRO DATABASES

Paper	Segment (ms)	Database	Classifier	Average Accuracy (%)
Geng et al. [22]	200	DB2	CNN[1]	77.80
Zhai et al. [17]	200 + 100	DB2	CNN	78.71
			SVM	77.44
		DB3	CNN	~57.00
			SVM	~55.00
Atzori et al. [23]	200	DB2	RF	75.27
		DB3	SVM	46.24*
This work	200 + 100	DB2	RF	75.88
			MLP	74.04
		DB3	RF	56.08
			MLP	53.06

[1] Convolutional Neural Network * Considering subject 7 from DB3

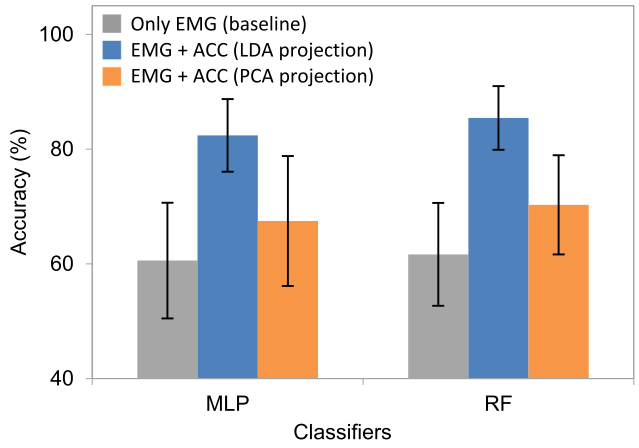

Fig. 11. Combining EMG with ACC.

CNN classifier, but our architecture is simpler and had less impact on processing time (presented in section III.B). Our results (for two classifiers) also indicated that the average classification accuracy for amputated subjects is 20% less than intact subjects and according to the existing literature [17, 23].

In order to increase the accuracy of the classifiers in DB2 and DB3 databases processing, a second offline assay was performed where we combined EMG and ACC data in multimodal classifier and we investigated the performance of pattern recognition. For these multimodal classifiers, the dimensionality reduction was performed with LDA and PCA methods to reduce the dimensionality of the feature vector and avoid overfitting in the classification step. The performance of this feature projection with MLP and RF classifiers for DB3 NinaPro database is compared and presented in Fig. 11. The assay was performed with 12 classes.

The experimental results show that combining EMG and ACC signals improves the recognition accuracy ($p < 0.01$) and also confirms the results obtained by Gijsberts *et al.* [24] and Fougner and collaborators [20] stating that inertial measurement data complemented the information for hand movement classification.

TABLE V
THE AVERAGE CLASSIFICATION ACCURACY (%) FOR DIFFERENT PAPERS COMBINING EMG AND ACC SENSORS

Paper	Number of classes	Sensors	Classifier	Average Accuracy (%)
Lv et al. [25]	5	8 EMG 8 ACC	RDA[2]	85.77
Krasoulis et al. [10]	6	16 EMG 16 ACC	LDA	95.0
Khushaba *et al.* [26]	6	6 EMG 3 ACC	SVM	90.0 ~ 91.0
This work	12	12 EMG 36 ACC	RF	90.13
			MLP	87.55

[2] Regularized Discriminant Analysis

In this work, for 12 classes, our best result was also with the LDA and RF approach that obtained an average classification accuracy of (85.44 ± 5.55)%. Combining LDA feature projection and MLP classifier the average accuracy was (82.40 ± 6.33)%. However, for classifiers with PCA feature projection, the average accuracy was less than 70%. This suggests that the approach lost some useful information from the EMG and ACC signals.

For intact subjects' database (DB2), we obtained accuracy rates with averages of (90.13 ± 3.08)% for RF multimodal classifier and (87.55% ± 2.63)% for MLP multimodal classifier. The (average) increase in recognition accuracy was 10% for the DB2 database and 21% for the amputee volunteers's database (DB3). We compared our classifiers with the existing literature (Table V).

Although the classification systems have different numbers of classes and sensors, it is possible to observe the classification level reached with the insertion of accelerometers.

Another analysis performed regards the customization level of the prosthesis. In this case, we evaluate the extent to which a prosthesis that uses a classifier already trained can predict the movements of a patient who still has not had their EMG signals used to train this prosthesis. The training and validation of classifiers with data from 10 volunteers and the test with data from another volunteer presented unsatisfactory results for all classifiers, with accuracy always under 30%. It occurs due to the influence of several factors in the EMG signals. Among them are the muscular fiber's diameter, the number of muscular fibers, the number of active motor units, the distance between the skin surface and the muscular fibers, the conduction speed, the blood flow in the muscle, the distance among electrodes, the relation between the type of fiber and its location and shooting rates of motor units [27]. The results show the need to create an acquisition routine of patients/users' EMG signals to train the prosthesis, enabling an individualized calibration activity.

B. Online System Results

For the database of local volunteers (KidoPro), the MLP classifier presented the best accuracy performances and was implemented on the SoC platform (Raspberry Pi 3 B+) with four TD functions: RMS, MAV, VAR and WL (the combination of feature projection and classifier did not improve accuracy). After communication and prediction tests, we evaluated the online system.

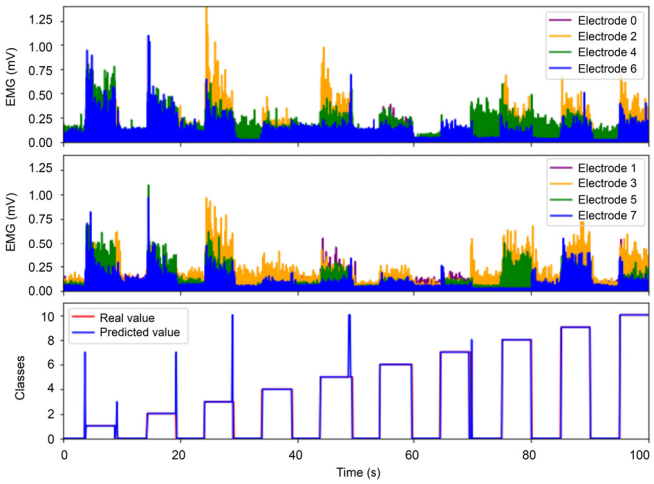

Fig. 12. Prediction performed by Raspberry platform.

In terms of classification metrics, every participant provided an accuracy above 95% (the best results were achieved by volunteer 4 with an average accuracy of 97.08% and the worst results were obtained by subject 3 with an average accuracy of 95.45%). The average accuracy of the MLP classifier was 96.30%. In our database, the results confirmed that there is a relationship between Body Mass Index (BMI) and classification accuracy. The results indicated that the accuracy increased significantly with the decrease in the volunteer's BMI. This result is in agreement with the studies presented by [16] in the NinaPro database, indicating that individuals with thicker adipose tissue decrease the amplitude and the signal-to-noise ratio of the EMG signal.

Figure 12 shows EMG signals of subject 2 and the comparison between the real values and the predicted values by the MLP classifier implemented on the Raspberry platform.

We can see in Fig. 12 that the greatest number of misclassifications occurs in the transitions of hand movements/gestures (movement onset and offset). For the prosthesis' electric actuation, this amount of movements was minimized through a simple routine presented in pseudo code 1.

Pseudo Code 1 Transition Detector and Adjustment Class Routine

Input: predict class Y_pred_{i-1} and Y_pred_i
Output: adjust class Y_adj
$flag = 0$
if Y_pred_i != Y_pred_{i-1}
    if ($flag==0$)
        $Y\_adj = Y\_pred_{i-1}$
        $flag = 1$
    else
        $Y\_adj = Y\_pred_i$
        $flag = 0$
else
    $Y\_adj = Y\_pred_i$
$Y\_pred_{i-1} = Y\_pred_i$

Figure 13 shows the system without the routine (a) with the transitions showing errors in the movements, while in (b) the result of the routine implemented with the reduction in the number of classified movements. However, there was no increase in the accuracy of movement classification and the total processing time is still less than 300 ms.

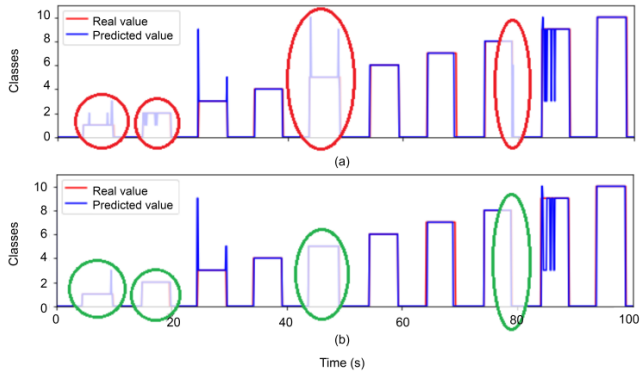

Fig. 13. Routine to minimize movements in the transition (subject 1).

The second test quantified the real-time system computation performance when operated on an embedded system. Fig. 14 shows the computation time of the different components of the real-time system. We used following metrics: the mean computation time (and standard deviation) and the maximal expected computation time within a 95% confidence interval assuming samples data with a normal Gaussian distribution. The pre-processing executed with a mean computation time of 1.61 $\pm$ 0.91 ms with 95% of the samples being computed within 3.44 ms. The features task executed with a computation time of 4.73 $\pm$ 0.63 ms (RMS: 0.88 $\pm$ 0.24 ms, MAV: 0.80 $\pm$ 0.13 ms, WL: 1.33 $\pm$ 0.40 ms and VAR: 1.71 $\pm$ 0.33 ms) with 95% of the samples being computed within 5.84 ms. The prediction component executed with a computation time of 4.59 $\pm$ 0.49 ms with 95% of the samples being computed within 5.7 ms. Total delay of these 3 stages of the system (pre-processing, features, prediction), executed with mean delay being 10.28 $\pm$ 1.81 ms and with 95% of the samples being produced within 13.29 ms.

We compared our system with the existing literature (Table VI), which presents classification systems between six to eleven classes.

From Table VI it can be seen that our system guarantees real-time response and has one of the lower response time. In terms of classification accuracy and considering the same number of classes ($k = 11$), our classifier obtained a result slightly lower than the value presented by Abbaspour *et al.* [5], but our processing time is 12 times less.

The shortest processing time was obtained by Raurale *et al.* [4], but they do not consider the pre-processing step. In our paper, excluding the pre-processing step, the response time is about 9 ms. Regarding classification accuracy above 99% obtained by [4], although with 9 classes, this is a goal in future studies.

We also present the kickstart of the force and slippage system for a prosthetic hand. In the grip assay, the prosthetic hand has been positioned on a support and directly commanded by the user. The tests were performed using three objects: a plastic cup, a tennis ball and a plastic rectangle. For the plastic cup (Fig. 15), the sequence of actions were: (a) prosthesis in the initial position and without the object; (b) prosthesis grasps the object; (c) the cup is filled with water.

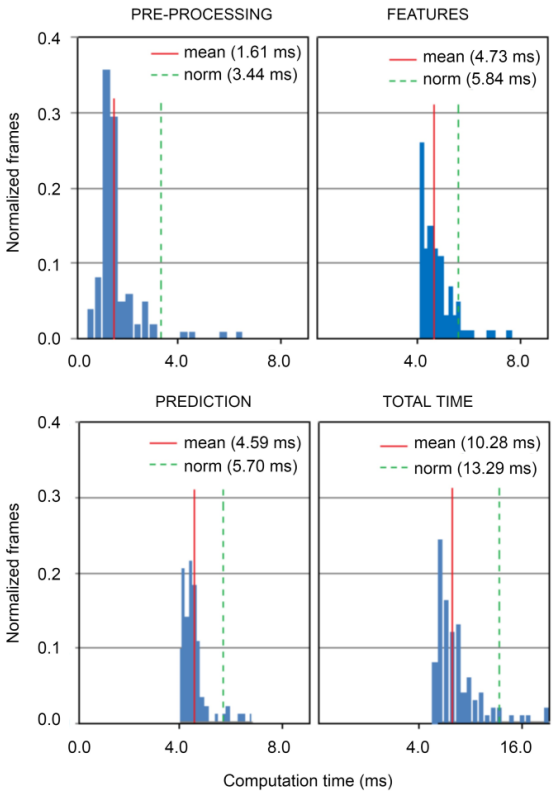

Fig. 14. Computation time on the Raspberry Pi.

TABLE VI
THE AVERAGE CLASSIFICATION ACCURACY (%) AND PROCESSING TIME

Paper	Classifier	Number of classes (k)	Accuracy (%)	Processing Time (ms)
Motoche and Benalcázar [28]	ANN	6	90.70	29.38
Sanchez-Velasco et al. [14]	EAM	8	95.83	-
Raurale et al. [4]	MLP	9	99.30	9.75
Abbaspour et al. [5]	MLE[3]	11	97.43	136.0
This work	MLP	11	96.30	10.28

[3]Maximum Likelihood Estimation

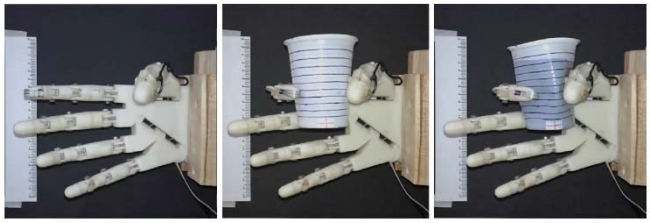

Fig. 15. Sequence of the grip and slip test (first object): (a) initial position and without object (b) holding object (c) filled with water.

The assays for the tennis ball (Fig. 16) and plastic rectangle (Fig. 17) consisted of the following sequence of actions: (a) prosthesis in the initial position and without the object; (b) prosthesis grasps the object; (c) a calibrated mass (weight of 200 g) is placed on object to evaluate the slip detection system and force application on the objects.

The results for the 30 trials have been performed with a success rate (i.e. number of compensated slippage event/number

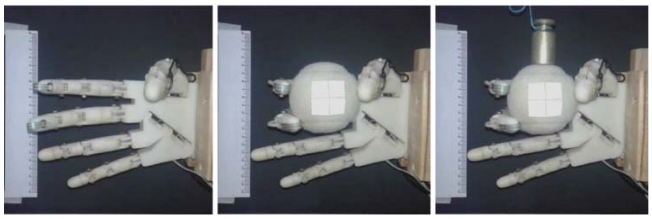

Fig. 16. Sequence of the grip and slip test (second object): (a) initial position and without object (b) holding object (c) applying calibrated mass.

Fig. 17. Sequence of the grip and slip test (third object): (a) initial position and without object (b) holding object (c) applying calibrated mass.

of trials) of 93.33% (the failures occurred two times in the third object). This value is similar to the result obtained by Cordella and collaborators [6] although in our experiment, we consider the actions "filling the cup" and "applying the calibrated mass on the object" as disturbances, keeping them during the process and in [6] the object slippage has been induced by applying an impulsive force to the object. Most of the studies used relatively static and/or constrained tasks (e.g., the ability to grasp and transfer a rigid object) and have not tested the feedback in force control during tasks across a range of different object size and weight.

In terms of slippage, Fig. 18 shows images of the test with plastic cup (without slip system and with slip system) and Fig. 19 and Fig. 20 present slip graphics of the cup.

Without the system (Fig. 18.a and Fig. 19), the plastic cup slides down approximately 45 mm until the cup rim touches the thumb and index finger of the prosthesis.

With the monitoring and control system (Fig. 18.b and Fig. 20), at t = 1.3 s, the cup starts to slide, the system detects the slip, generating a signal for more force to be applied on the object. With the application of more force, the cup rises to the +2.5 mm position (t = 1.8 s). As the volume of water in the plastic cup increases until it is completely filled, it slides to the -2.6 mm position (t = 5.0 s). With the detection and control system, the cup slides 5.1 mm (39.9 mm less than the system without slip detection).

The use of slip sensors caused considerable deformation of the plastic cup, but it did not compromise system performance. At this point, a balance between the applied force and the slip must be performed through new assays.

On average, the ball slipped 2.5 mm and the rectangle object slipped 5.6 mm.

Although the results of the classification of the hand gestures and the object grip tests were applied, we observed some hardware limitations and possible system improvements. The first problem is the hand prosthesis used and its limitations are described by Tian *et al.* [29]. They used the same open-source prosthesis design in their experiments. The main limitations

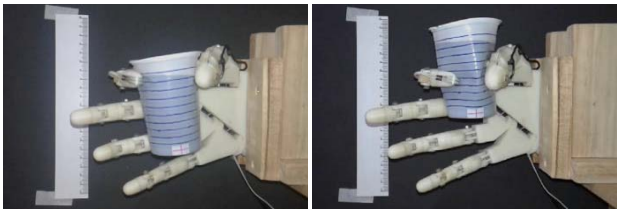

Fig. 18. Holding and slipping test of the object.

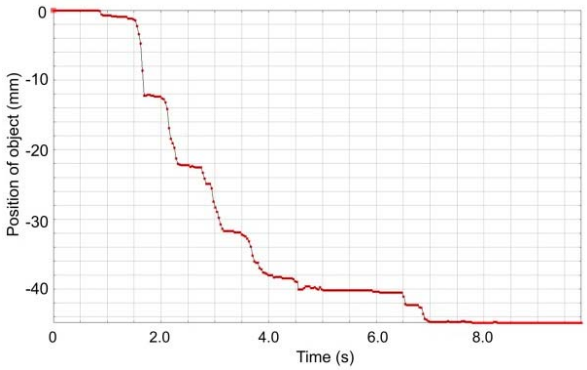

Fig. 19. Results with plastic cup without slip sensor.

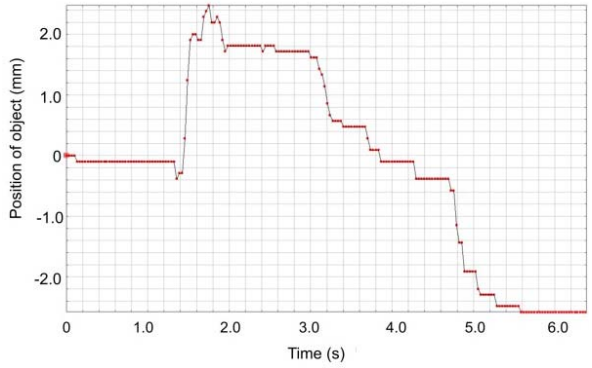

Fig. 20. Results with plastic cup with slip system.

described by them and which also impacted our experiments were: the force that the five motors can produce is lower than the grip strength of the human hand (we have limitation of gripping heavy objects); the type of material of the prosthesis (PLA) is unable to withstand such high force and limits also heavy objects gripping; the surface of 3D printed robotic hand is solid and smooth (it is hard to create enough friction when holding a heavy object). This last item was responsible for the failures occurred in our assays. To improve this adherence between the objects and the prosthesis, future experiments will be performed with the coverage of the fingers and palm with silicone material as showed in [8, 30] and also inserting the silicone glove in the prosthetic hand as presented in [6, 29], evaluating the system performance for each proposal. Future works will also be proposed with other objects and other grasp configurations.

The second point concerns the limitation of EMG signal acquisition devices. We believe that this issue needs to be further investigated in order to design effective systems for control of upper limb prosthesis. Raurale and collaborators [4] suggest the data fusion of EMG sensors with other sensors, for, instance, gyroscope and accelerometer in order to reduce EMG channels without significant reductions in capability. The described system could be performed by wearable acquisition devices.

IV. Conclusion

In this paper, we explored two aspects about studies on the control of upper limb prosthesis: EMG pattern recognition system and sensory feedback system. A complete hardware/software system to classify EMG signals, which responds under the limited time defined for real-time use (300 ms) was presented. The accuracy of the classifier and time response are comparable to the results obtained in other state of art papers. We also implemented in robotic fingers a multimodal sensor system for gripping objects.

Future studies in online systems include the following experiments: acquisition of accelerometry signals and generation of a new database for multimodal classifiers (data fusion between EMG and ACC sensors for classification of hand movements); integration of ACC sensors with force and slip sensors in object gripping systems according to the first studies presented by Weiner *et al.* [6]. In addition, we can consider experiments with more subjects (healthy and amputees), prosthesis' actuation tests with new mechanical system design and a prosthesis calibration system, grip tests of different objects and the movement of these objects from one place to another as presented by Liow *et al.* [30].

Supplementary Materials

Github repository (include database, Python scripts from onset detection and offline experiments and movies of some assays): https://github.com/eng-olegario/prosthesis-control

Fig. S1: Schematic diagram of the force sensor signal conditioner.

Fig. S2: Schematic diagram of the slip sensor signal conditioner.

Movie S1: Grasping of plastic cup (with slip system).

Movie S2: Grasping of plastic cup (without slip system).

Movie S3: Grasping of tennis ball (with slip system).

Movie S4: Grasping of tennis ball (without slip system).

Movie S5: Grasping of plastic rectangle (with slip system).

Movie S6: Grasping of plastic rectangle (without slip system).

Others: Python scripts and KidoPro database.

References

[1] M. H. Stoppa and J. C. M. Carvalho, "Kinematic modeling, motion simulation, construction and control of hand prosthesis for handling tasks," in *Proc. Math. Appl. Ind., Problems Solution Methods. Blucher*, 2016, pp. 183–208.

[2] G. K. Patel, C. Castellini, J. M. Hahne, D. Farina, and S. Dosen, "A classification method for myoelectric control of hand prostheses inspired by muscle coordination," *IEEE Trans. Neural Syst. Rehabil. Eng.*, vol. 26, no. 9, pp. 1745–1755, Sep. 2018.

[3] M. Cognolato, M. Atzori, C. Marchesin, S. Marangon, D. Faccio, and C. Tiengo, "Multifunction control and evaluation of a 3D printed hand prosthesis with the myo armband by hand amputees," *BioRxiv*, vol. 1, pp. 445–460, Jan. 2018.

[4] S. A. Raurale, J. McAllister, and J. M. del Rincon, "Real-time embedded EMG signal analysis for wrist-hand pose identification," *IEEE Trans. Signal Process.*, vol. 68, pp. 2713–2723, 2020.

[5] S. Abbaspour, M. Lindén, H. Gholamhosseini, A. Naber, and M. Ortiz-Catalan, "Evaluation of surface EMG-based recognition algorithms for decoding hand movements," *Med. Biol. Eng. Comput.*, vol. 58, no. 1, pp. 83–100, Jan. 2020.

[6] P. Weiner, C. Neef, Y. Shibata, Y. Nakamura, and T. Asfour, "An embedded, multi-modal sensor system for scalable robotic and prosthetic hand fingers," *Sensors*, vol. 20, no. 1, p. 101, Dec. 2019.
[7] L. Zollo *et al.*, "Restoring tactile sensations via neural interfaces for real-time force-and-slippage closed-loop control of bionic hands," *Sci. Robot.*, vol. 4, no. 27, Feb. 2019, Art. no. eaau9924.
[8] F. Cordella *et al.*, "A force-and-slippage control strategy for a poliarticulated prosthetic hand," in *Proc. IEEE Int. Conf. Robot. Autom. (ICRA)*, May 2016, pp. 3524–3529.
[9] A. Prakash and S. Sharma, "A low-cost system to control prehension force of a custom-made myoelectric hand prosthesis," *Res. Biomed. Eng.*, vol. 36, no. 3, pp. 237–247, Sep. 2020.
[10] A. Krasoulis, S. Vijayakumar, and K. Nazarpour, "Multi-grip classification-based prosthesis control with two EMG-IMU sensors," *IEEE Trans. Neural Syst. Rehabil. Eng.*, vol. 28, no. 2, pp. 508–518, Feb. 2020.
[11] W.-T. Shi, Z.-J. Lyu, S.-T. Tang, T.-L. Chia, and C.-Y. Yang, "A bionic hand controlled by hand gesture recognition based on surface EMG signals: A preliminary study," *Biocybern. Biomed. Eng.*, vol. 38, pp. 126–135, Jan. 2018.
[12] F. Gaetani, G. A. Zappatore, P. Visconti, and P. Primiceri, "Design of an arduino-based platform interfaced by Bluetooth low energy with myo armband for controlling an under-actuated transradial prosthesis," in *Proc. Int. Conf. IC Design Technol. (ICICDT)*, Jun. 2018, pp. 185–188.
[13] N. Y. Sattar, U. A. Syed, S. Muhammad, and Z. Kausar, "Real-time EMG signal processing with implementation of PID control for upper-limb prosthesis," in *Proc. IEEE/ASME Int. Conf. Adv. Intell. Mechatronics (AIM)*, Jul. 2019, pp. 120–125.
[14] L. E. Sánchez-Velasco, M. Arias-Montiel, E. Guzmán-Ramírez, and E. Lugo-González, "A low-cost EMG-controlled anthropomorphic robotic hand for power and precision grasp," *Biocybern. Biomed. Eng.*, vol. 40, no. 1, pp. 221–237, Jan. 2020.
[15] M. Atzori *et al.*, "Electromyography data for non-invasive naturally-controlled robotic hand prostheses," *Sci. Data*, vol. 1, no. 1, Dec. 2014, Art. no. 140053.
[16] M. Atzori *et al.*, "Characterization of a benchmark database for myoelectric movement classification," *IEEE Trans. Neural Syst. Rehabil. Eng.*, vol. 23, no. 1, pp. 73–83, Jan. 2015.
[17] X. Zhai, B. Jelfs, R. H. M. Chan, and C. Tin, "Self-recalibrating surface EMG pattern recognition for neuroprosthesis control based on convolutional neural network," *Frontiers Neurosci.*, vol. 11, p. 379, Jul. 2017.
[18] S. Solnik, P. Rider, K. Steinweg, P. DeVita, and T. Hortobágyi, "Teager–Kaiser energy operator signal conditioning improves EMG onset detection," *Eur. J. Appl. Physiol.*, vol. 110, no. 3, pp. 489–498, Oct. 2010.
[19] A. Phinyomark, F. Quaine, S. Charbonnier, C. Serviere, F. Tarpin-Bernard, and Y. Laurillau, "EMG feature evaluation for improving myoelectric pattern recognition robustness," *Expert Syst. Appl.*, vol. 40, no. 12, pp. 4832–4840, 2013.
[20] A. Fougner, E. Scheme, A. D. C. Chan, K. Englehart, and O. Stavdahl, "A multi-modal approach for hand motion classification using surface EMG and accelerometers," in *Proc. Annu. Int. Conf. IEEE Eng. Med. Biol. Soc.*, Aug. 2011, pp. 4247–4250.
[21] A. Tharwat, T. Gaber, A. Ibrahim, and A. E. Hassanien, "Linear discriminant analysis: A detailed tutorial," *AI Commun.*, vol. 30, no. 2, pp. 169–190, 2017.
[22] W. Geng, Y. Du, W. Jin, W. Wei, Y. Hu, and J. Li, "Gesture recognition by instantaneous surface EMG images," *Sci. Rep.*, vol. 6, no. 1, Dec. 2016, Art. no. 36571.
[23] M. Atzori, M. Cognolato, and H. Müller, "Deep learning with convolutional neural networks applied to electromyography data: A resource for the classification of movements for prosthetic hands," *Frontiers Neurorobotics*, vol. 10, p. 9, Sep. 2016.
[24] A. Gijsberts, M. Atzori, C. Castellini, H. Muller, and B. Caputo, "Movement error rate for evaluation of machine learning methods for sEMG-based hand movement classification," *IEEE Trans. Neural Syst. Rehabil. Eng.*, vol. 22, no. 4, pp. 735–744, Jul. 2014.
[25] B. Lv, X. Sheng, W. Guo, X. Zhu, and H. Ding, "Towards finger gestures and force recognition based on wrist electromyography and accelerometers," *Proc. Int. Conf. Intell. Robot. Appl.*, 2017, pp. 373–380.
[26] R. N. Khushaba, A. Al-Timemy, S. Kodagoda, and K. Nazarpour, "Combined influence of forearm orientation and muscular contraction on EMG pattern recognition," *Expert Syst. Appl.*, vol. 61, pp. 154–161, Nov. 2016.
[27] G. Kamen and G. E. Caldwell, "Physiology and interpretation of the electromyogram," *J. Clin. Neurophysiol.*, vol. 13, no. 5, pp. 366–384, Sep. 1996.
[28] C. Motoche and M. E. Benalcázar, "Real-time hand gesture recognition based on electromyographic signals and artificial neural networks," in *Proc. 27th Int. Conf. Artif. Neural Netw.*, Rhodes, Greece, vol. 8131, 2018, pp. 352–361.
[29] L. Tian, N. Magnenat Thalmann, D. Thalmann, and J. Zheng, "The making of a 3D-printed, cable-driven, single-model, lightweight humanoid robotic hand," *Frontiers Robot. AI*, vol. 4, p. 65, Dec. 2017.
[30] L. Liow, A. B. Clark, and N. Rojas, "OLYMPIC: A modular, tendon-driven prosthetic hand with novel finger and wrist coupling mechanisms," *IEEE Robot. Autom. Lett.*, vol. 5, no. 2, pp. 299–306, Apr. 2020.

João Olegário de Oliveira de Souza received the B.S. degree in electrical engineering and the M.S. degree in applied computing from Unisinos University, in 2007 and 2013, respectively, where he is currently pursuing the Ph.D. degree in applied computing. He is a Professor with Unisinos University. His main research interests include robotics and artificial intelligence systems.

Marcos Daniel Bloedow received the B.S. degree in electrical engineering from Unisinos University in 2017. He is a Software and Hardware Developer with Commbox Tecnologia. His research interests include embedded systems, robotic, and instrumentation.

Felipe Cezimbra Rubo received the B.S. degree in electronics engineering from Unisinos University in 2020. He graduated as an Electronics Technician at Liberato Salzano Vieira da Cunha Technical School Foundation in 2013. He is a Research and Development Software Supervisor at Altus Sistemas de Automação S.A. His main research interests include embedded systems and software development.

Rodrigo Marques de Figueiredo received the B.S. degree in electrical engineering, the M.S. degree in applied computing, and the Ph.D. degree in remote sensing applied to geology from Unisinos University, in 2005, 2009, and 2016, respectively. His research interests include robotics and telecommunication.

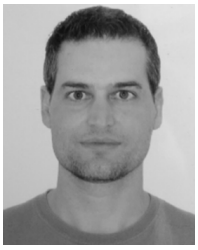

Gustavo Pessin received the D.Sc. degree in computer science from the University of São Paulo. He was a member of the Mobile Robotics Lab. He is currently a Full Researcher within the Robotics Laboratory, Vale Institute of Technology. The bulk of his research interests are related to intelligent systems and mobile robots.

Sandro José Rigo (Member, IEEE) is a Professor with Unisinos University. He is aslo a Researcher with the Applied Computing Graduate Program, a Consultant on Innovation and Information Technology, and research project coordinator. His fields of interest are artificial intelligence, educational data mining, semantic web, and natural language processing.